Generation of NPS for Exposure Experiments from Copper Acetylacetone.

Moravec, Pavel
2016

GENERATION OF NPS FOR EXPOSURE EXPERIMENTS FROM COPPER ACETYLACETONATE

Pavel MORAVEC[1], Jaroslav SCHWARZ[1], Petr VODIČKA[1], Jaroslav KUPČÍK[1,2], Jaroslav ŠVEHLA[1]

[1]Institute of Chemical Process Fundamentals of the CAS, v.v.i., Prague, Czech Republic, moravec@icpf.cas.cz
[2]Institute of Inorganic Chemistry of the CAS, v.v.i., Husinec-Řež, Czech Republic, kupcik@iic.cas.cz

Keywords: Copper acetylacetonate, Hot wall reactor, MOCVD, Nanoparticle generation, Exposure experiments

INTRODUCTION

Particles containing copper are emitted from smelters, iron foundries, power stations, and municipal incinerators (WHO, 1998) and also from brake linings during breaking, Kukutschová *et al.* (2011). Nanoparticles (NPs) of copper are ingredients in polymers, inks, and bioactive coatings inhibiting the growth of microorganisms, Cioffi at al. (2005), and CuO NPs has been used in antimicrobial textiles, Gabbay and Borkow (2006), therefore they can be easily inhaled. Even though CuO NPs were found highly toxic, Karlsson et al. (2008), in vivo studies of their toxicity are still rather rare. In this work we tested a method of long lasting nanoparticle generation from copper acetylacetonate (CuAA) for use in follow up exposure experiments with laboratory animals. The exposure chamber for inhalation experiments was constructed in the Institute of Analytical Chemistry AS CR (Večeřa et al., 2011) and some methods of NPs generation for these experiments were already tested in our laboratory (Moravec et al., 2015, Moravec et al., 2016).

EXPERIMENTAL SETUP

Experiments were performed in an externally heated work tube with i. d. 25 mm and the length of heated zone 1 m. Total length of the work tube made from impervious aluminous porcelain (IAP) was 1.5 m. Inlet section arrangements for thermal decomposition of CuAA vapours in an inert atmosphere (pyrolysis) and in the mixture of nitrogen and air (oxidation) are shown in Figure 1. In this study, only the results of CuAA pyrolysis are presented. The particle production and characteristics were studied in dependence on reactor temperature (T_R), reactor flow rate (Q_R) and precursor vapour pressure (P_{CuAA}). P_{CuAA} was controlled by the saturator temperature (T_S) and saturator flow rate (Q_S) and its values in the saturator were calculated from the equation (Nassibulin et al., 2001):

$$P_{CuAA}(Pa) = 1000 \times 10^{\left(7.641 - \frac{41707}{T_S(K)}\right)}, \quad (1)$$

valid in the temperature range from 80 to 190 °C. Experimental setup was described in more detail by Moravec et al. (2015). Particle production in the form of particle size distribution was monitored with a scanning mobility particle sizer (SMPS, TSI model

3936L75) and the samples for particle characterization were deposited onto Ni TEM grids, covered with C-foil, using a nanometer aerosol sampler (NAS, TSI model 3089) and on cellulose, quartz, Zefluor and Sterlitech Ag filters. The particle characteristics were studied with high resolution transmission electron microscopy (HRTEM, *JEOL 3010*, samples on TEM grids), energy dispersive spectroscopy (EDS, *INCA/Oxford* connected to *JEOL 3010*, TEM grids), inductively coupled plasma – optical emission spectrometry (ICP-OES, *Agilent 4200 MP-AES,* cellulose filters) and X-ray diffraction (XRD, *Bruker D8 Discover diffractometer*, Ag filters). Interpretations of selected area electron diffraction (SAED) patterns were performed using program ProcessDiffraction (Lábár, 2008, Lábár, 2009).

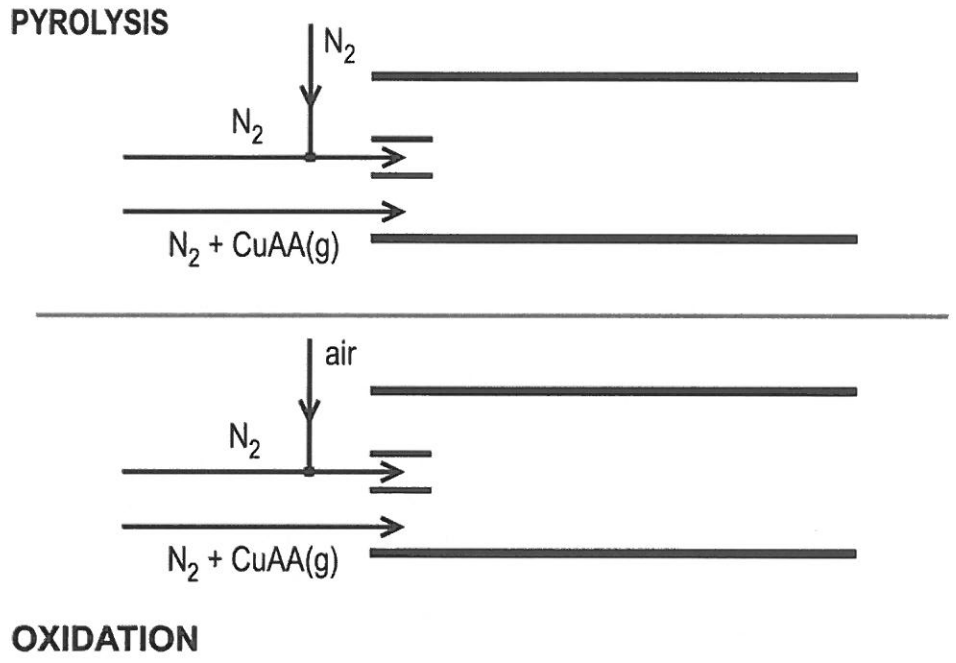

Fig. 1: Scheme of the inlet section arrangements for pyrolysis and oxidation of CuAA.

RESULTS AND CONCLUSIONS

NPs production was studied during one experimental campaign with duration of 102 h and it is shown in dependence on experimental parameters T_R (500–700 °C), T_S (120–133.5 °C), Q_R (800–1200 cm³/min) and Q_S (80 – 150 cm³/min, i.e. 10-12.5 vol. % of Q_R) in Figure 2. Particle production in Figure 2 is represented by number total concentration N_t and geometric mean diameter GMD, but we have also available NPs production in mass total concentration M_t (μg/m³) and surface total concentration S_t (nm²/cm³). It can be seen, that NPs production can be controlled by precursor vapour pressure P_{CuAA} (controlled by T_S and Q_S; NPs production increases with P_{CuAA}) and depends also on T_R and Q_R (NPs production increases in the range of investigated experimental conditions both with T_R and Q_R). NPs production was stable at steady state conditions with N_t high above 1x10⁷ #/cm³. Total mass concentrations were calculated for the standard value of particle density 1.2 g/cm³ in Aerosol Instrument Manager software. This value might seem to be far from the density of copper or copper oxide, but it has to be taken into account that SMPS detects agglomerates of primary particles in our experiments, and therefore exaggerates the real total volume of detected NPs.

Therefore this approximation seems to be appropriate in most cases. Mass concentrations from SMPS measurements varied from 460 to 830 μg/m³ at T_R=500 °C, 1600 to 3000 μg/m³ at T_R=600 °C, and 1700 to 2000 μg/m³ at T_R=700 °C, but at T_R=700 °C, the value of P_{CuAA} was lower (0.14 Pa) than at T_R=600 °C (0.20 Pa). Mass concentrations from filter measurements varied in the same order of T_R from 390 to 890 μg/m³, 1900 to 2800 μg/m³, and 3700 to 4000 μg/m³, respectively. We can see, that at T_R=700 °C mass concentrations from filter measurements are twice as high as the values from SMPS, which can be apparently attributed to more dense NPS and/or NPs agglomerates at T_R=700 °C. Emission rates from SMPS measurements varied from 1.4 to 9.0 μg/min, while from filters measurements from 1.2 to 12.1 μg/min.

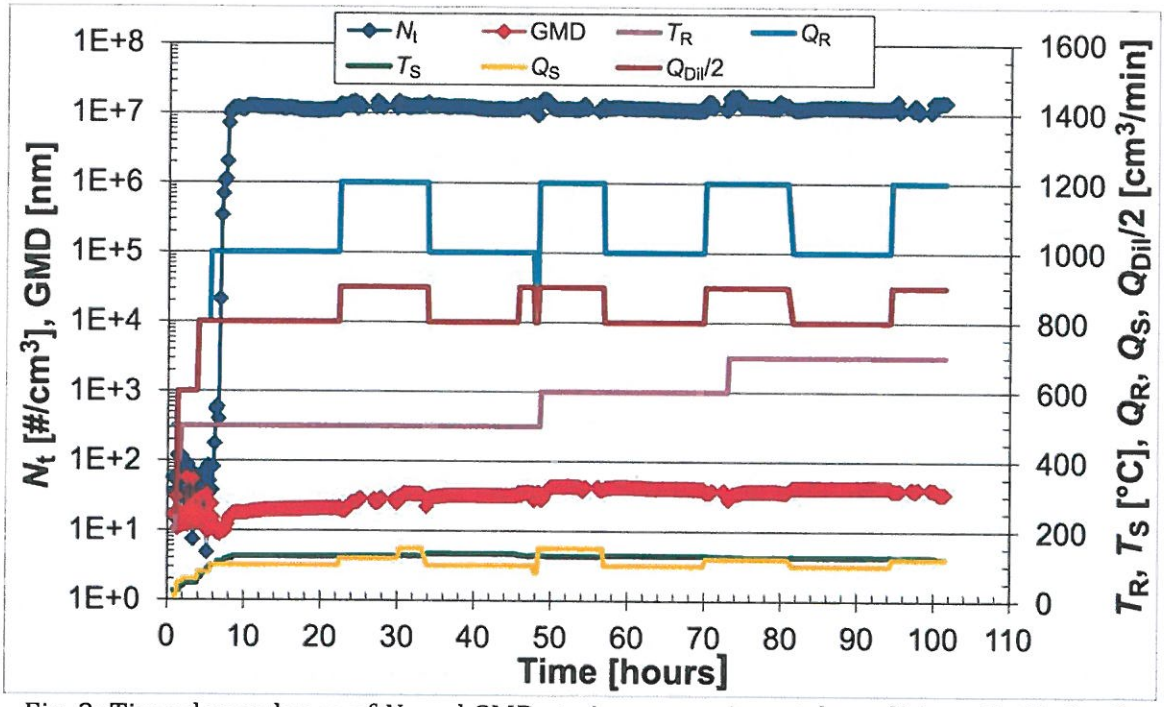

Fig. 2: Time dependence of N_t and GMD at given experimental conditions T_R, T_S, Q_R, Q_S and $Q_{dil/2}$.

Morphology of NPs was studied using HRTEM and an example of HRTEM images of the sample synthesized at T_R=500 °C can be seen in Figure 3. Primary particles are mostly spherical, agglomerated into clusters of various sizes and the size of primary particles varies typically in the range from 5 to 10 nm. The size of NPs synthesized at T_R 600 and 700 °C was a bit larger, typically from 5 to 15 nm.

EDS analyses detected elements Cu, O, C and Ni. Here Ni originates from TEM grid, C mostly from grid foil and partially from carbonaceous side products of precursor decomposition, captured in the NPs during their formation. An average O to Cu ratio (atomic %) was close to 1, but oxygen can originate also from grid foil and side products of precursor decomposition, so that it is difficult to deduce an oxidic form of Cu in NPs from the results of EDS analyses. Concentration of Cu in the samples on cellulose filters was analysed by ICP-OES method on the emission line 324.754 nm: the content of Cu was 47.3 mass % in the sample synthesized at 500 °C and 72.9 % in the sample synthesized at 700 °C. EC/OC analyses of the samples deposited on quartz fibre filters showed that the content of total carbon (TC) was 20.1, 10.1 and 9.0 mass % in the samples synthesized at 500, 600 and 700 °C, and from those values the content EC

accounted for 8.9, 6.4 and 6.6 mass %. That means that NPs prepared at T_R 600 and 700 °C contain 10 or less mass % of TC.

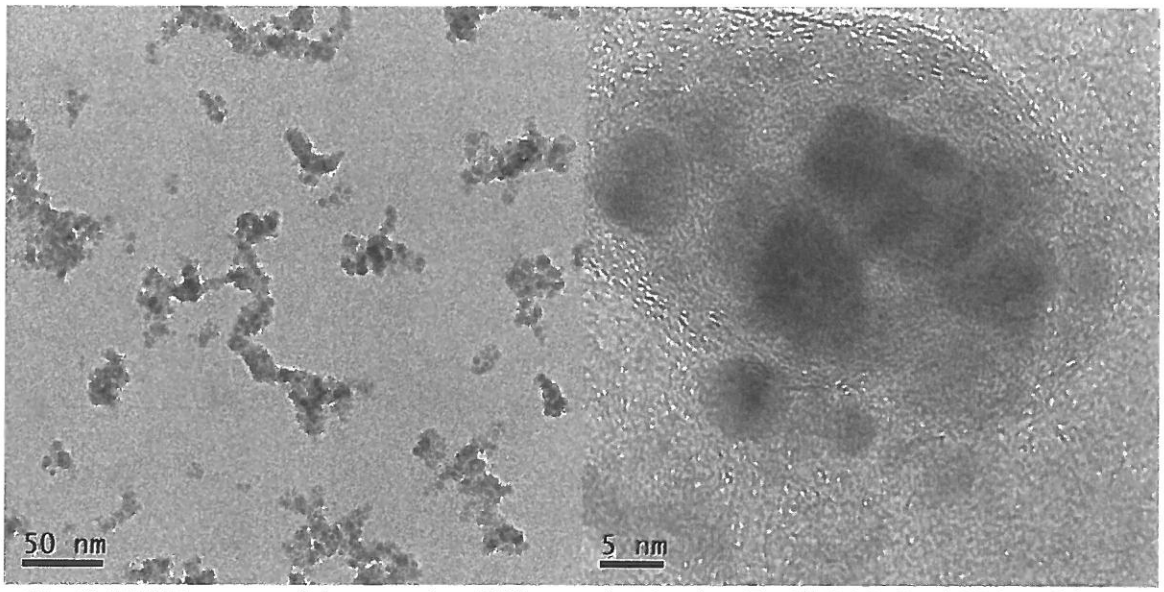

Fig. 3: TEM images of the sample of NPs synthesized at T_R=500 °C, Q_R=1200 cm³/min, T_S=127 °C, Q_S=120 cm³/min, Q_{Dil}=1800 cm³/min.

XRD analysis identified NPs generated at T_R=500 °C as XRD amorphous. In the samples generated at T_R 600 and 700 °C, XRD method identified crystalline structure of cubic Cu, PDF 85-1326. Besides metallic Cu, in the sample synthesized at 700 °C, also traces of cuprite (Cu_2O) crystalline phase, PDF 74-1230, were identified. Mean crystallite sizes in these samples, calculated by integral breadth method (LVol-IB), were 5.4 and 6.1 nm, respectively. These values are in quite a good agreement with primary particle sizes detected by HRTEM. SAED method identified crystalline phase also in NPs synthesized at T_R=500 °C, which can be seen in Figure 3 (lattice fringes), but especially from electron diffraction in Figure 4.

Electron diffraction pattern in Figure 4 is quite weak and (outer) rings are rather diffusive, but diffraction pattern was identified as a mixture of cubic Cu and cubic Cu_2O crystalline structures. Electron diffraction patterns of NPs generated at T_R 600 and 700 °C are much better developed, but in principle confirmed the same. However, the ratio of cubic Cu to cubic Cu_2O crystallites is increasing with increasing T_R.

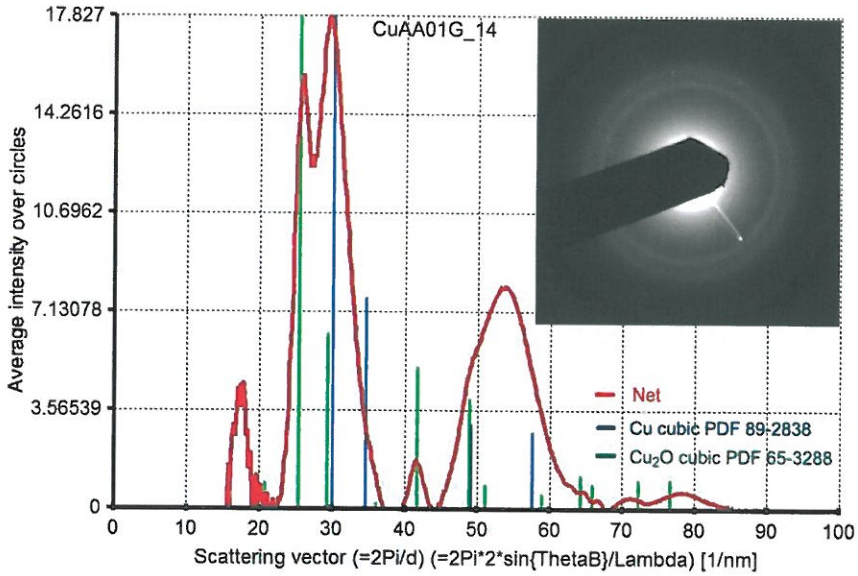

Fig. 4: Comparison of electron diffraction pattern of NPs synthesized at T_R=500 °C, Q_R=1200 cm³/min, T_S=127 °C, Q_S=120 cm³/min, Q_{Dil}=1800 cm³/min (inset and red curve) with model diffractions of cubic Cu and cubic Cu_2O.

In conclusion, the generation of NPs by CuAA thermal decomposition in an inert atmosphere at T_R= 700 °C seems to be the favourable method for long lasting exposure experiments with laboratory animals. The particle production rate is sufficiently high (up to 4000 μg/m³) and can be further increased by an increase of T_S or/and Q_S, and it is stable at steady state conditions for sufficiently long time. The primary particle size is very small, so that they have very high surface area, which is the biologically most effective matrix for acute nanoparticle toxicity in the lung, Schmid and Stoeger (2016). Moreover, the NPS have well defined characteristic. The content of Cu in NPs is 73 mass %, predominantly in the form of metallic Cu, and they contain only 9 mass % of TC.

ACKNOWLEDGEMENT

This work was supported by the Czech Science Foundation under grant P503/12/G147. XRD analyses were performed by Mgr. Anna Kallistová, Geological Institute of the CAS, v.v.i.

REFERENCES

Cioffi N., Ditaranto N., Torsi L., Picca R. A., Sabbatini L., Valentini A., Novello L., Tantillo G. et al. Analytical characterization of bioactive fluoropolymer ultra-thin coatings modified by copper nanoparticles, *Anal. Bioanal. Chem.*, 381, 607-616, (2005).

Gabbay J., Borkow G. Copper oxide impregnated textiles with potent biocidal activities, *J. Ind. Text.*, 35, 323-335, (2006).

Karlsson H. L., Cronholm P., Gustafsson J., Möller L. Copper oxide nanoparticles are highly toxic: A Comparison between metal oxide nanoparticles and carbon nanotubes, *Chem. Res. Toxicol.*, 21, 1726-1732, (2008).

Kukutschová J., Moravec P., Tomášek V., Matějka V., Smolík J., Schwarz J., Sejdlerová J., Šafářová K., Filip P. On airborne nano/micro-sized wear particles released from low-metallic automotive brakes, *Environmental Pollution* 159, 998-1006, (2011).

Lábár J.L. Electron diffraction based analysis of phase fractions and texture in nanocrystalline thin films; Part I: Principles, *Microscopy and Microanalysis* 14, 287-295, (2008).

Lábár J.L., Electron diffraction based analysis of phase fractions and texture in nanocrystalline thin films; Part II: Implementation, *Microscopy and Microanalysis* 15, 20-29 (2009).

Moravec P., Smolík J., Ondráček J., Vodička P., Fajgar R. Lead and/or lead oxide nanoparticle generation for inhalation experiments, *Aerosol. Sci. Technol.*, 49, 655-665, (2015).

Moravec P., Schwarz J., Vodička P., Koštejn M. Study of TiO_2 nanoparticle generation for follow-up inhalation experiments with laboratory animals, *Aerosol. Sci. Technol.*, DOI: 10.1080/02786826.2016.1224803; (2016).

Nasibulin A. G., Ahonen P., Richard O., Kauppinen E. I., Altman I. S. Copper and copper oxide nanoparticle formation by chemical vapor nucleation from copper(II) acetylacetonate, *J. Nanoparticle Res.*, 3, 385-400, (2001).

Schmid O., Stoeger T. Surface Area is the Biologically Most Effective Dose Metric for Acute Nanoparticle Toxicity in the Lung, *J. Aerosol Sci.*, 99, 133–143, (2016).

Večeřa Z., Mikuška P., Moravec P., Smolík J. Unique exposure system for the whole body inhalation experiments with small animals. Nanocon 2011, 21.-23.9.2011, Brno, Czech Republic, pp 652-654.

WHO (1998) Environmental Health Criteria for Copper, No. 200, International Programme on Chemical Safety, World Health Organisation, Geneva, Switzerland.